EFFECT OF ROTARY SWAGING ON STRESS/STRAIN STATE WITHIN TUNGSTEN HEAVY ALLOY BAR

[1]Ludmila KRÁTKÁ, [1]Sergei KISELEV

[1]VSB - Technical University of Ostrava, Ostrava, Czech Republic, EU,
ludmila.kratka@vsb.cz, sergej.kiselev@vsb.cz

https://doi.org/10.37904/metal.2021.4113

Abstract

Owing to their exceptional combination of mechanical and physical properties, tungsten heavy alloys (THAs) are advantageous for demanding applications. The presented study focuses on analysing the effects of processing of THA bar by the cold rotary swaging method, particularly on investigating the effects of processing on residual stress within the swaged bar. The stress-state was predicted numerically using the finite element method (FEM) and the results were subsequently validated using data acquired experimentally via scanning electron microscopy (SEM-EBSD). As shown by the results, the predicted parameters corresponded well with the experimentally acquired data; by the effect of the swaging process, the effective imposed strain was the highest at the surface of the bar and decreased towards its axis, which corresponded to the distribution of microhardness, as well as the detected residual stress distribution. Nevertheless, the study focused on preliminary swaging experiment consisting of two swaging passes; the predicted results impart that the stress/strain gradient will diminish with continuing swaging.

Keywords: Rotary swaging, numerical simulation, structure analysis, mechanical properties

1. INTRODUCTION

Tungsten heavy (pseudo) alloys (THA) are produced using powder metallurgy. Mixed metal powders of the prescribed size are isostatically pressed in various ways into rods. In the next step, the bars are sintered in a protective atmosphere (H, Ar, vacuum), in the temperature range 1000 – 1500 °C. Add other alloying elements with lower melting values (Ni, Co, Mo, Re) to the powder mixtures with lower melting point and better plastic properties, which creates a matrix around the tungsten grains during sintering by melting the boundaries. In this way, a homogeneous material is formed [1,2].

In our case, it is a pseudo-alloy W-Ni-Co. These alloys are characterized by their high tungsten content (min. 90 % by weight), which surrounds softer NiCo matrices. These alloys are sought after for their high strength (maximum strength up to 1900 MPa). THAs are widely used in industries as protection against harmful radiation or to block kinetic energy. The preferred use of THA is, for example, in medicine as a shields in the manufacture of therapeutic devices in oncology. Another use of THA is, for example, in aviation as a counterweight in aviation technology, or for the production of kinetic penetrators used by the military. These applications use a high density of THA (≈16 g/cm³) [3-5].

Rotary swaging (RS) seems to be a suitable technology for THA processing, which results from the already published issue [6-8]. Rotary swaging is an advantageous technology for the processing of solid semi-finished products or also for the production of hollow shaped parts. RS is used for processing difficult to process materials such as Ti, THA. It also enables the production of composite materials (Al / Cu) thanks to the advantageous stress distribution of forces during rotary swaging [9,10].

A number of publications have addressed the issue of stress states and deformation behaviour during MS. The works shows that the plastic flow during cold and hot rotary swaging differs significantly in its course.

In cold rotary swaging, it is evident that additional tangential stresses play an important role in the case of plastic flow and stress distribution in the material. Residual stress is a very important indicator of rotary swaging, which subsequently affects the mechanical properties of THA products. Publications on this topic are relatively rare because not enough attention has been paid to this issue [11,12].

This study is primarily focused on the analysis of stress states and residual stresses in cold swaged tungsten rods. In the first part we focus on stress prediction using finite element methods (FEM) simulation. The numerical simulation program FORGE NxT was used for this purpose. In the second part, we focus on the experimental verification of residual stresses in the material, which took place after processing the material using rotary swaging.

2. MATERIAL AND METHODS

In the first part we focus on FEM simulation of the process of rotary swaging of material performed cold way. In this way, the data of the designed rotary swaging process are verified. In the study we focus on the prediction of stress states in connection with the material flow. In the second part we focus on the real application of predicted rotary swaging (see **Figure 1**). The rotary swaging itself took place on a rotary swaging machine from the HMP company.

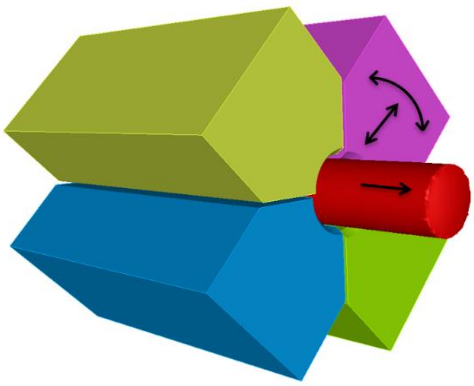

Figure 1 Scheme of rotary swaging

The FEM simulation of the rotary swaging was designed to predict the behaviour of the heavy tungsten alloy WNiCo. An elastic-viscoplastic model created by software was used to predict the deformation behaviour. The model is created on the basis of the stress-strain curve in THA tension. The model was determined by the Hensel - Spittel relation (see equation (1)), where $\dot{\varepsilon}$ (s^{-1}) is the equivalent strain rate, ε (-) is the equivalent strain, T (K) is the temperature and A, m_1, m_2, m_3, m_4, m_5, m_7, m_8, m_9 are regression coefficients, whose values were as follows: A = 1447.00273, m_1 = -0.009, m_2 = 0.089, m_3 = 0.0044, m_4 = -0.0069, m_5, m_7, m_8, m_9 were 0.

$$\sigma = A\cdot \exp(m_1\cdot T)\cdot T^{m_9}\cdot \varepsilon^{m_2}\cdot \exp\left(\frac{m_4}{\varepsilon}\right)\cdot (1+\varepsilon)^{m_5\cdot T}\cdot \exp(m_7\cdot \varepsilon)\cdot \dot{\varepsilon}^{m_3}\cdot \dot{\varepsilon}^{m_8\cdot T} \quad (1)$$

The pseudo-alloy selected for the experiment was WNiCo, with a chemical composition of 90 wt. % W, 7 wt. % Ni, 3 wt. % Co (determined by SEM-EDX analysis), was prepared from selected metal powders with a mean grain size of 2.78 µm. The process of preparation of pseudo-alloys takes place in steps: 1. mixing of powders, 2. isostatic cold pressing at 400 MPa and 3. sintering at 1525 °C for 20 minutes in a protective atmosphere (H) followed by controlled cooling in the furnace and final cooling in water (hardening). This preparation procedure was performed in Mabave s. r. o.

Cold rotary swaging technology was used to process the semi-finished products. Rotary swaging took place in two steps, where the initial diameter (30 mm) of the material was slightly asymmetric and then swaged into a rod with a diameter of 20 mm. The bars on cross-sectional sections were subjected to scanning electron microscopy (SEM-EBSD) after swaging, and we further focus on the development of the (sub) structure. EBSD analyses were performed in the subsurface sample area.

3. RESULTS AND DISCUSSION

3.1. FEM Analysis of rotary swaging

Figure 2 shows the flow of material with a projected temperature field during cold rotary swaging. The simulation shows that the material flow is complicated during rotary swaging. It can be seen that the material flows in the direction of the rotary swaging throughout the process. The material flows most significantly when entering the reduction zone. It is steamy from the figure that the material flow in the reduction zone gradually changes. Towards the end of the reduction zone, we see a visible rotation around the material axis. This phenomenon is caused by the tangential component of the plastic flow and also indicates the formation of a rigid end in this area, which significantly affects the material flow. In the part where the material is already behind the working part of the dies, it is evident from the vector arrangement that the material tends to bend in these places. The figure also shows how much heating due to deformation heat occurs during cold rotary swaging.

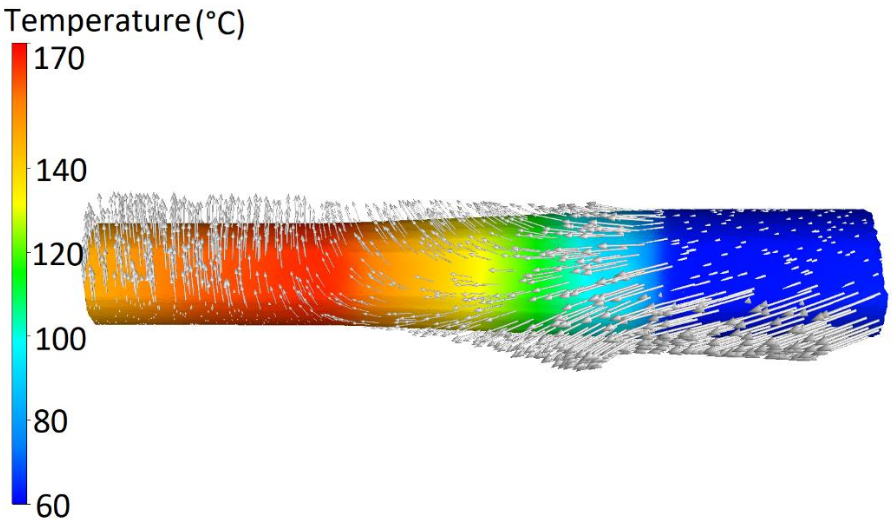

Figure 2 Temperature field in the longitudinal direction

In **Figure 3a)** a stress state is shown, which takes into account both normal and shear stresses in the material during rotary swaging. Compressive stresses dominate in the surface layers. This phenomenon is mainly caused by friction between the anvils and the material. In this subsurface layer, the material flow is lower due to the lower plasticity. This area is thus rather a carrier of plastic deformation towards the centre of the semi-finished product. This leads to compressive stresses. Compressive stresses are manifested in the subsurface areas, which causes better conditions for the flow of material. These tensile stresses show that the greatest movement of material occurs in these places. The compressive stress is displayed again in the centre of the material. These compressive stresses result from the nature of the material flow during rotary swaging. There is not enough deformation in the central area and the material does not have enough energy to flow. A significant part of the plastic flow is realized in the subsurface layers. Therefore, the axial regions of the sample are characterized by the compressive character of the stress.

In **Figure 3b)** the main normal tensile stresses are shown. The **Figure 3b)** shows that the tensile stresses are concentrated in the sub-surface area. **Figure 3c)** shows the main normal compressive stresses. In this view, the effect of compression in the middle and surface area of the material is significantly manifested.

The resulting **Figure 3d)** is an intersection of **Figure 3b)** and **Figure 3c)** it follows that the normal compressive stresses are only slightly suppressed by tensile stresses in the central region.

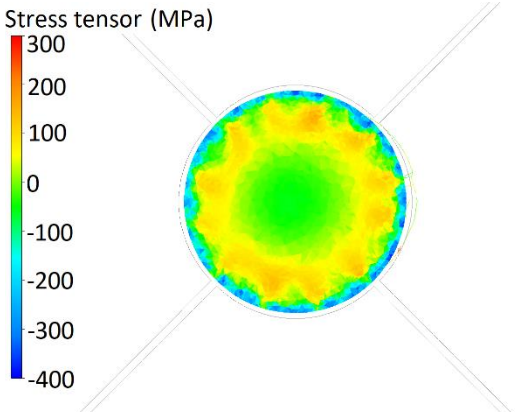

a) Stress tensor

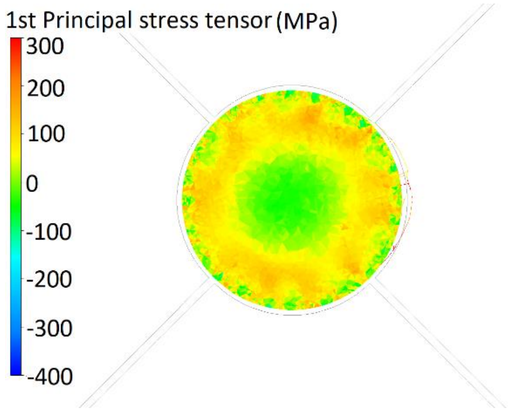

b) 1st Principal stress tensor

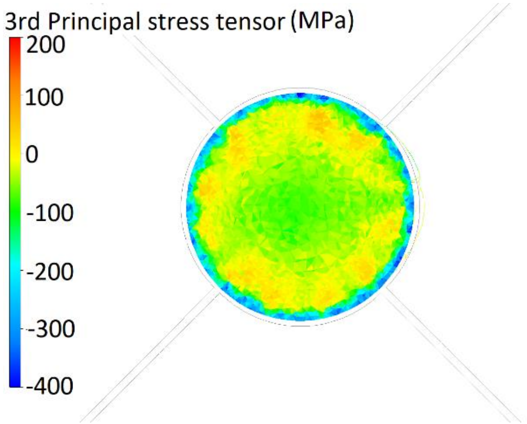

c) 3rd Principal stress tensor

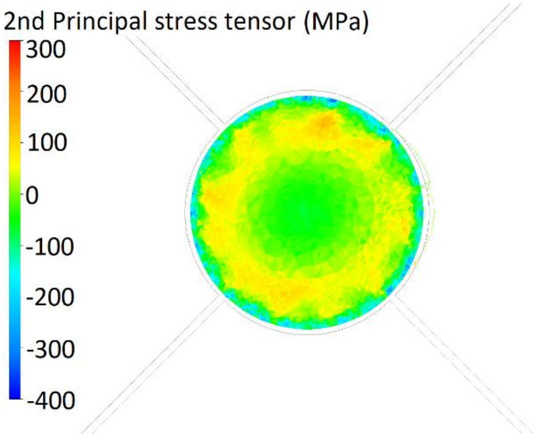

d) 2nd Principal stress tensor

Figure 3 Stress state in the cross section of cold swaged material

It follows from this distribution of tensile and compressive stresses (see **Figure 3**) that the stress state during cold forging of the material has a rather compressive character in most of the cross-sections. Thus, this character indicates that the material does not have sufficient energy to flow. This is caused by the high deformation resistance, which results in a significant strengthening of the material.

3.2. Structural analysis and residual stress

Figure 4a) shows the state after sintering, where large spherical tungsten grains are surrounded by a softer NiCo matrix. This matrix ensures the integrity of the material as well as its plastic properties. **Figure 4b)** and **Figure 4c)** shows the structural state after cold rotary swaging. In **Figure 4b)** shows a subsurface area where a higher penetration of deformation occurs. This phenomenon is evident from the deformation of the matrix and the slight deformation of the tungsten grains. In many areas, the matrix is deformed so that the tungsten grains appear to touch. In **Figure 4c)** the centre of the sample is shown and it is steamy that there is no such significant penetration of deformation. The deformation is concentrated in the NiCo matrix region at this point. Therefore, we see almost no deformed tungsten grains at this point.

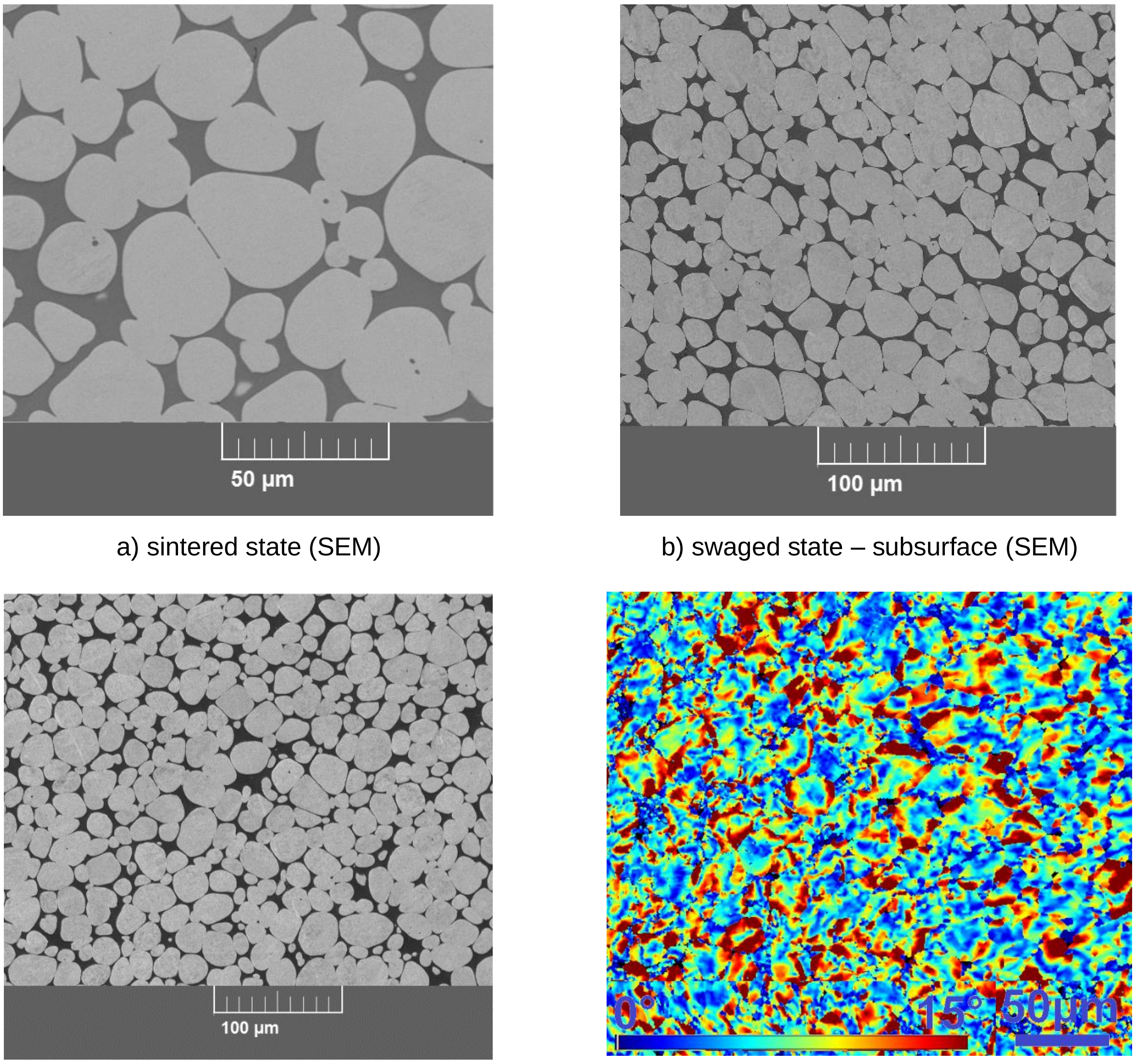

a) sintered state (SEM)

b) swaged state – subsurface (SEM)

c) swaged state – centre (SEM)

d) internal grains orientations in axial region of swaged material (SEM-EBSD)

Figure 4 SEM structure of swaged alloy and SEM-EBSD swaged alloy

Figure 4d) shows the orientation of the grains in the surface area of the material. This orientation shows us in which places there will be residual stress. In the red areas, the tungsten grains are most mis-oriented and touch each other. They do not have space to relax in these places. The result is the highest residual stress. The blue areas largely correspond to the arrangement of the matrix in the material, or to areas with a very similar grain orientation. In these places there is the lowest residual stress, because the tungsten grains eat space for relaxation. During deformation, the mis-orientation of the grains decreases due to deformation and in this way residual stress is created in the material. This development of stress is characteristic of the deformation behaviour during the rotary swaging.

4. CONCLUSIONS

In rotary swaging, the material flow is very complicated. The phenomenon of the existence of a rigid end is significantly manifested here, which is significantly manifested in the front part of the material during real rotary swaging and causes bending of the material. The stress in the material during cold rotary swaging is characterized in most of the cross-section by a compressive character. The flow of material during cold rotary swaging is not so significant, which is characterized by a lower proportion of tensile stresses across the cross section. The temperature distribution in the material according to the results from FEM indicates a significant increase in the temperature of the material due to the heat of deformation. Structural analyses confirm the occurrence of additional shear stresses in the material in the subsurface layer. The structure is more deformed compared to the central areas. There is no such significant deformation in the central area. The deformation in these areas is concentrated in the matrix area.

ACKNOWLEDGEMENTS

This research was supported by the 19-15479S project of the Grant Agency of the Czech Republic.

REFERENCES

[1] ESSAM, M., ELSAYED, A., SHASH, A., ADLY, M. Fabrication of tungsten heavy alloy long rods by warm powder extrusion and vacuum sintering. *Journal of Materials Research and Technology*. 2019, vol. 8, no. 2, pp. 2209-2215.

[2] SENTHILNATHAN, N., RAJA, A.A., VENKATACHALAM, G. Sintering of Tungsten and Tungsten Heavy Alloys of W–Ni–Fe and W–Ni–Cu: A Review. *Transactions of the Indian Institute of Metals*. 2017, vol. 70, pp.1161-1176.

[3] KUNČICKÁ, L., KOCICH, R., KLEČKOVÁ, Z. Effects of Sintering Conditions on Structures and Properties of Sintered Tungsten Heavy Alloy. *Materials*. 2020, vol. 13, no. 10, 2338.

[4] HAFIZOĞLU, H., DURLU, N. Effect of sintering temperature on the high strain rate-deformation of tungsten heavy alloys. *International Journal of Impact Engineering*. 2018, vol. 121, pp. 44-54.

[5] DAS, J., APPA, R.G., PABI, S.K. Microstructure and mechanical properties of tungsten heavy alloys. *Materials Science and Engineering: A.* 2010, vol. 527, pp. 7841-7847.

[6] KOCICH, R., KUNČICKÁ, L., DOHNALÍK, D., MACHÁČKOVÁ, A., ŠOFER, M. Cold rotary swaging of a tungsten heavy alloy: Numerical and experimental investigations. *International Journal of Refractory Metals and Hard Materials*. 2016, vol. 61, pp. 264-272.

[7] YU, Y., ZHANG, W., CHEN, Y., WANG, E. Effect of swaging on microstructure and mechanical properties of liquid-phase sintered 93W-4.9(Ni, Co)-2.1Fe alloy. *International Journal of Refractory Metals and Hard Materials*. 2014, no. 44, pp. 103-108.

[8] KATAVI, B., ODANOVIĆ, Z., BURZIĆ, M. Investigation of the rotary swaging and heat treatment on the behavior of W- and γ-phases in PM 92.5W–5Ni–2.5Fe–0.26Co heavy alloy. *Materials Science and Engineering: A*. 2008, vol. 1-2, no. 492, pp. 337-345.

[9] ZHANG, Q., JIN, K., MU, D., MA, P., TIAN, J. Rotary swaging forming process of tube workpieces. **In:** *11th International Conference on Technology of Plasticity, ICTP 2014.* Japan: Procedia Engineering, 2014, vol. 81, pp. 2336-2341.

[10] KOCICH, R., KUNČICKÁ, L., KRÁL, P., STRUNZ, P. Characterization of innovative rotary swaged Cu-Al clad composite wire conductors. *Materials and Design*. 2018, vol. 160, pp. 828-835.

[11] KUNČICKÁ, L., MACHÁČKOVÁ, A., LAVERY, N.P., KOCICH, R., CULLEN, J.C.T., HLAVÁČ, M. Effect of thermomechanical processing via rotary swaging on properties and residual stress within tungsten heavy alloy. *International Journal of Refractory Metals and Hard Materials*. 2020, vol. 87, no. 105120.

[12] KUNČICKÁ, L., KOCICH, R., HERVOCHES, CH., MACHÁČKOVÁ, A. Study of structure and residual stresses in cold rotary swaged tungsten heavy alloy. *Materials Science and Engineering: A*. 2017, vol. 704, pp. 25-31.